Effect of the Degree of Branching on Atomic-Scale Free Volume in Hyperbranched Poly[3-ethyl-3-(hydroxymethyl)oxetane]. A Positron Study

Wei Gong,[†] Yiyong Mai,[‡] Yongfeng Zhou,[‡] Ning Qi,[†] Bo Wang,*[,†] and Deyue Yan*[,‡]

Department of Physics, Wuhan University, 430072, China, and College of Chemistry and Chemical Engineering, Shanghai Jiao Tong University, Shanghai 200240, China

Received May 19, 2005; Revised Manuscript Received June 23, 2005

ABSTRACT: Positron annihilation lifetime (PAL) measurements have been used to study the effect of degree of branching (DB) and temperature on the atomic-scale free-volume properties and the structural transitions for hyperbranched polymer PEHO. According to the finite-term positron lifetime analysis and differential scanning calorimeter (DSC) measurements, the glass transition temperature was determined, which indicates that the higher the DB, the lower the glass transition temperature, and the higher the concentration of free-volume hole. Change in dispersion of the free volume shows that, with DB increase, there might be a disappearance of the dynamic heterogeneity in highly branched PEHO and a transition to homogeneous mass may take place. It is very interesting to observe the existence of two long-lived components (τ_3 and τ_4) above T_g using the continuous lifetime analysis, which suggests that two kinds of different structures appear including a local ordered region and an amorphous region due to the molecular chains motion, indicating that an effective rearrangement of chains can take place, i.e., paracrystalline regions formed above T_g related to the packing density of chains.

Introduction

Hyperbranched polymers (HBPs) are a relatively new class of macromolecules, which have gained significant attention from both academia and industry in recent years, owing to the potential new properties of their highly branched, highly functionalized, three-dimensional globular structure.[1,2] Many excellent studies about this have been published.[3−9] However, most of them paid more attention to the synthesis, modification, and characterization of functional hyperbranched polymers with special properties, and few reports concern the microstructure, i.e., atomic-scale free-volume holes in hyperbranched polymers.

It is well-known that the microstructure and nanoscale level voids can significantly affect the physical properties of polymers, such as the mechanical properties and diffusion phenomena. Hence, measurements of free volume in hyperbranched polymers, in particular holes at atomic level, are of prime importance not only for scientific exploration but also for potential engineering applications.

Positron annihilation lifetime spectroscopy (PALS) is considered to be the most direct method to probe the interior cavity space in polymers. It is based on the fact that the lifetimes of positron and its bound forms—positronium (Ps)—are sensitive to the existence of structural inhomogeneities, because the formation and annihilation of positronium (bound state of e^+ and e^-) is localized in nano- or subnanoscale level holes.[10−14]

The positron annihilation lifetime technique is a powerful method to estimate the free-volume parameters in the amorphous region of polymers. A orthopositronium (o-Ps: the triple bound-state of positronium of a positron and an electron) probe has a relatively small diameter (0.106 nm) and a repulsive nature compared with the atoms and molecules in a substance; thus one can obtain information on defect, atomic vacancy, void, nanocage, and free volume, much more sensitively and exactly than information from other methods. The free-volume parameters have been utilized to explore a change of physic-chemical properties such as glass transition, thermal expansion, and structural relaxation at lower temperature in polymers. Furthermore, a free-volume distribution, which associates with a nanoscopic inhomogeneity, was utilized in the study of the distribution of free volume.[12]

In the present work, the microstructure of the hyperbranched polymer PEHO was studied by the positron annihilation lifetime measurement. Effects of degree of branching and temperature on the glass transition and distribution of the free volume have been discussed.

Experimental Part

Samples. Poly[3-ethyl-3(hydroxymethyl)oxetane] (PEHO) samples with different degrees of branching (DBs) were synthesized according to the procedure described in the literature.[15] The schematic architectures of mostly linear PEHO and hyperbranched PEHO with a higher DB are illustrated in Figure 1. D, L, and T units stressed in Figure 1B respectively express the dendritic, the linear, and the terminal units of branched PEHO, which determine the DBs of different PEHO samples. Figure 2 shows the ^{13}C NMR spectra of PEHO samples from 20.5 to 24.5 ppm. The three well-separated peaks respectively belong to the carbon atoms of methylene in the ethyl groups of D units, L units, and T units. DBs of different PEHO samples can be calculated by integration of the areas of the three peaks,[16,17] and the results are listed in Table 1. T_gs of the samples,[18] measured by a differential scanning calorimeter (DSC), are also given in Table 1. Details of the samples can be found in the previous work.[15]

Positron Lifetime Measurements. Positron lifetime measurements were carried out by using a conventional fast−fast coincidence system with a time resolution of ~270 ps (fwhm) determined by ^{60}Co prompt resolution data. A 30 μCi ^{22}Na positron source sealed in two aluminum foils (0.8 mg cm^{-2}) was placed between two pieces of the same sample. γ-rays with energies of 1.27 MeV (emitted from β-decay of the ^{22}Na source) and 0.511 MeV (emitted from positron annihilation in the

* Corresponding authors: (B.W.) bwang@positron.whu.edu.cn; (D.Y.) dyyan@sjtu.edu.cn.
[†] Wuhan University.
[‡] Shanghai Jiao Tong University.

10.1021/ma051026j CCC: $30.25
Published on Web 09/07/2005

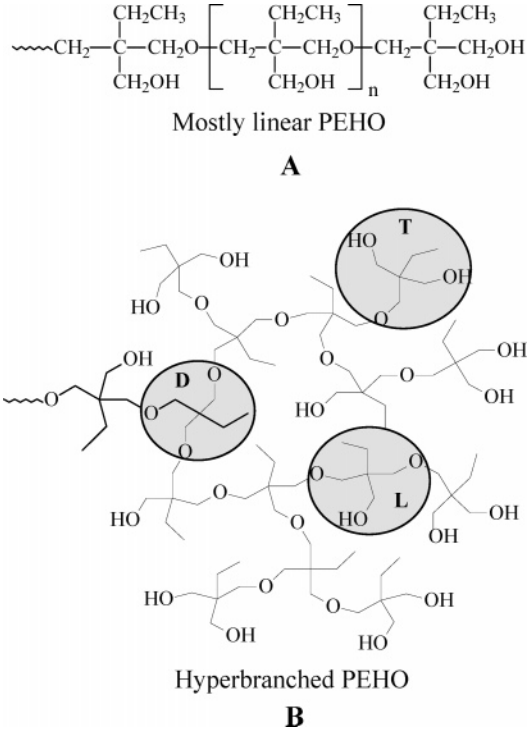

Figure 1. Structures of mostly linear PEHO (A) and hyperbranched PEHO (B).

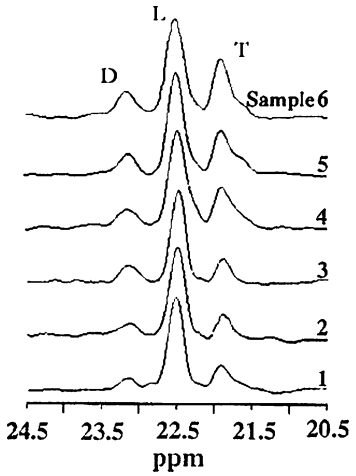

Figure 2. ^{13}C NMR spectra of PEHO samples.

Table 1. Characterizations of PEHO Samples

sample name	PEHO1	PEHO2	PEHO3	PEHO4	PEHO5	PEHO6
DB (%)	9	11	15	22	36	41
T_g (K)	337.0	334.8	329.0	326.2	316.2	310.9

sample) were detected by detectors as the start and the stop impulse signals, respectively. Samples for PALS measurement were in a form of small disks with diameters of 10 mm and thickness of 1.5 mm. To minimize the artifact, charging of each sample is performed in the same position as marked.

PAL measurements have been performed in the temperature range from 150 to 380 K. Temperature of samples was determined and stabilized with an accuracy of ±1 K using a liquid nitrogen cryostat. Each spectrum contained approximately one million and four million counts for PATFIT[19] and MELT,[20–22] and the collecting time for each is about 1.5 and 6.0 h, respectively. Analyses of positron lifetime spectra were performed using the continuous analysis technique (maximum entropy lifetime method) MELT program and finite-term lifetime analysis PATFIT program. Moreover, to reduce artificial effects, spectra were resolved using the same parameters.

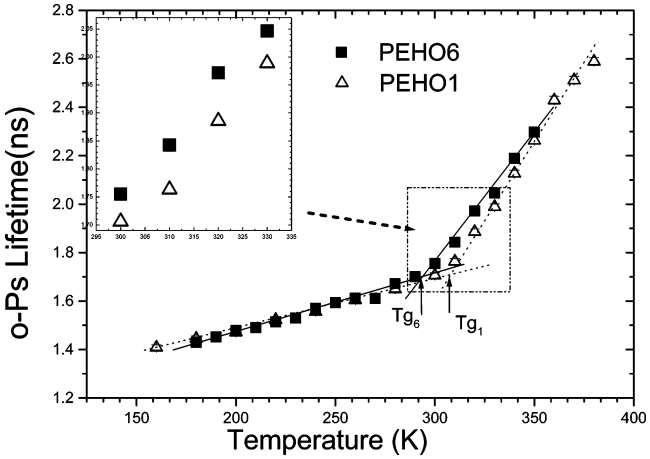

Figure 3. Temperature dependence of the o-Ps lifetime.

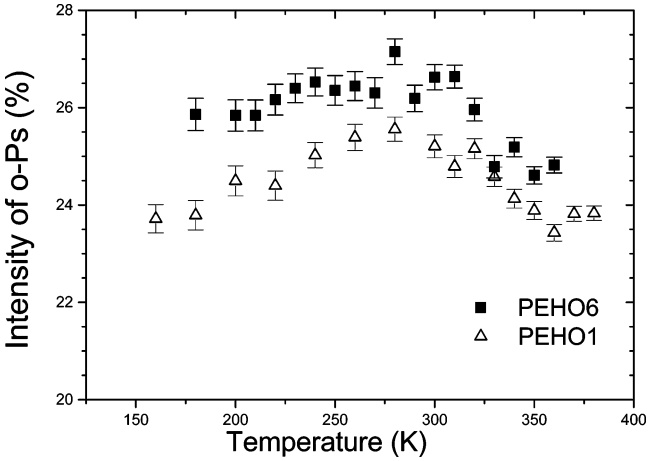

Figure 4. Temperature dependence of the o-Ps intensity.

Data Analysis. Positron lifetime spectra were best fitted with three components using PATFIT. The shortest-lived component τ_1 (~0.15 ns) is attributed to the self-annihilation of parapositronium and "free" positron annihilation. The intermediate-lived component, $\tau_2 = 0.40 \pm 0.02$ ns, is assigned to annihilation of positron trapped in various vacancies. The longest-lived component, τ_3 (~1.2−2.8 ns), is attributed to the o-Ps pick-off annihilation in free-volume holes in amorphous region According to the simplified free-volume model, the average radius R of free-volume holes can be evaluated from τ_3, as described in eq 1[23]

$$\tau_{o-Ps} = \frac{1}{2}\left[1 - \frac{R}{R_0} + \frac{1}{2\pi}\sin\left(\frac{2\pi R}{R_0}\right)\right]^{-1} \quad (1)$$

where τ_{o-Ps} is o-Ps lifetime (ns), R is the size (radius) of free-volume holes (Å), and $R_0 = R + \Delta R$ where $\Delta R = 1.66$ Å[24] is an empirical electron layer thickness. The intensity of o-Ps, I_3, is supposed to be linearly dependent on the concentration of free-volume holes. The fractional free-volume F_v can be expressed as $F_v = CI_{o-Ps}V_f$, where $V_f = (4/3)\pi R^3$ is the average volume of free-volume hole (assuming spherical geometry). For convenience, we define a relative fractional free-volume $F_r = I_{o-Ps}V_f$.

Since only the long-lived o-Ps lifetimes could be related to the properties of the pores in the samples, the following discussions are mainly based on the annihilation characteristics of the long-lived components.

Results and Discussion

Glass Transition Process. Temperature dependences of o-Ps lifetime and its intensity for two PEHO samples are shown in Figures 3 and 4, respectively. The mean lifetime τ_3 of the o-Ps increases with increasing

temperature, which suggests an increase of the free-volume size. The relative intensities I_3 for both PEHO samples increase gradually to a maximum and then decrease with the increase of temperature.

Obviously, the slope $d\tau_3/dT$ does not remain the same throughout the temperature range investigated, indicating the existence of a structural transition. To determine the structural transition temperature, a least-squares linear fitting of the straight line may be used to approximate the temperature dependence of the o-Ps lifetime. An empirical relation between o-Ps lifetime and temperature can be linearly fitted within two temperature regions as follows:

PEHO1:

$$\tau_3(T) = 1.4084 + 4.5678 \times 10^{-3}T\,(\text{ns}) \quad (160 \le T \le 300\ \text{K}) \quad (2)$$

$$\tau_3(T) = 1.8332 + 1.0576 \times 10^{-2}T\,(\text{ns}) \quad (310 \le T \le 380\ \text{K}) \quad (3)$$

PEHO6:

$$\tau_3(T) = 1.4297 + 2.2258 \times 10^{-3}T\,(\text{ns}) \quad (180 \le T \le 280\ \text{K}) \quad (4)$$

$$\tau_3(T) = 1.7012 + 9.022 \times 10^{-3}T\,(\text{ns}) \quad (290 \le T \le 360\ \text{K}) \quad (5)$$

Taking the intersections of the two segments as the glass transition temperature, 310 and 290 K can be identified as T_g, respectively. It is evident that the higher the DB, the lower the T_g, which is in good agreement with those values obtained from DSC. The evidence given in Figure 3 indicates that the initiation of the "micro-Brownian" motion is more favorable for the highly branched PEHO. Generally, the glass transition temperature determined by PALS is about 25 K lower than that measured by DSC. This is because the measurement of positron lifetime spectroscopy at each temperature requires over an hour (polymer is in quasi-equilibrium state), while the measurement by DSC takes less than a minute[25−27] (polymer is in a nonequilibrium state). Below and near T_g, the long-time relaxation progress may affect significantly the molecular structure of polymers, in particular, the relaxation of molecular chains, which led to the difference in T_g measured by PALS and DSC.

From Figure 4, we can see that I_3 shows a slight increase of 7.93% for PEHO6 and 8.62% for PEHO1 before 280 K, and then it decreased gradually. This phenomenon has also been observed in physical aging.[28] According to the report,[29] it is complex to explain the variation in o-Ps intensity with temperature, because the radiation effect of e^+ irradiation on o-Ps formation probability in nonpolar is different from in polar polymer. In polar polymers, the effect of positron irradiation can be neglected. Thus, for polar molecules of PEHO, the variations in o-Ps intensity could be mainly attributed to the changes in free-volume holes, since the o-Ps intensity I_3 is considered to be linearly dependent on the number of free-volume holes.

The thermodynamic process can be divided into two stages by T_g: glassy state and rubbery state. In the former stage, both the o-Ps lifetime and the o-Ps intensity increase with increasing temperature. Such a phenomenon has been found in several polymers.[30−32] A possible explanation is that the "fast motion" that has a localized and cage character is frozen; this means that the o-Ps has a greater chance of being localized in free volume, which brings about an increase in formation probability of o-Ps. On the other hand, the slight increase in τ_3 below T_g is based on the increase in local chain motion and the rotation of the methyl group in glassy state. Above T_g, the increase in τ_3 mainly stems from the release of micro-Brownian motion of the whole chains and the formation of bigger free-volume holes descending from the combination of small ones. Simultaneously, the decrease in I_3 indicates a decrease in the number density of holes (supposing I_3 is linearly dependent on the concentration of free-volume holes). These results can be explained as follows: first, when $T > T_g$, the "fast motion" may be activated, and thus the o-Ps has less chance of being localized in free-volume, which results in slight decrease of I_3; second, the combination of smaller holes to form larger free-volume voids can also apparently reduced the free-volume number, which is in good agreement with the increase of o-Ps lifetime.

Effect of DB on the Microstructure of PEHO. From Figure 3, it is clear that the o-Ps lifetime τ_3 for both hyperbranched polymers are almost the same below 290 K. When 290 K $< T <$ 350 K, τ_3 in PEHO6 increases more dramatically than that in PEHO1; when $T >$ 350 K, there is hardly any difference between the two samples in τ_3. Figure 4 reveals that the numerical intensity of free-volume holes in highly branched PEHO6 is larger than that in less branched PEHO1 throughout the temperature range studied.

Figure 5 shows the changes of relative free-volume fraction with temperature, F_r is of bigger value in PEHO6 than that in PEHO1; an empirical relation between F_r and temperature can be linearly fitted within two temperature regions as follows:

PEHO1:

$$F_r(T) = 11.01 + 4.7048 \times 10^{-2}T \quad (160 \le T \le 300\ \text{K}) \quad (6)$$

$$F_r(T) = 20.2297 + 2.2279 \times 10^{-1}T \quad (300 \le T \le 380\ \text{K}) \quad (7)$$

PEHO6:

$$F_r(T) = 12.4241 + 5.0667 \times 10^{-2}T \quad (180 \le T \le 280\ \text{K}) \quad (8)$$

$$F_r(T) = 18.6579 + 1.8596 \times 10^{-1}T \quad (290 \le T \le 360\ \text{K}) \quad (9)$$

We can also divide the process into two segments by T_g. Below T_g, the slope dF_r/dT of the two samples is almost the same; however, when $T > T_g$, the slope dF_r/dT in PEHO6 is obviously different in PEHO1.

It has been reported that the higher the degree of branching, the shorter the average length of chains between two branching points. It is reasonable to suppose that the various molecular motions require different expenditures of energy, and consequently, they are activated in different amounts at fixed temperature, which results in the difference of τ_3 between the two samples during the temperature range from 290 to 350 K above T_g. The higher value of the free-volume density for the highly branched PEHO6 suggests that free

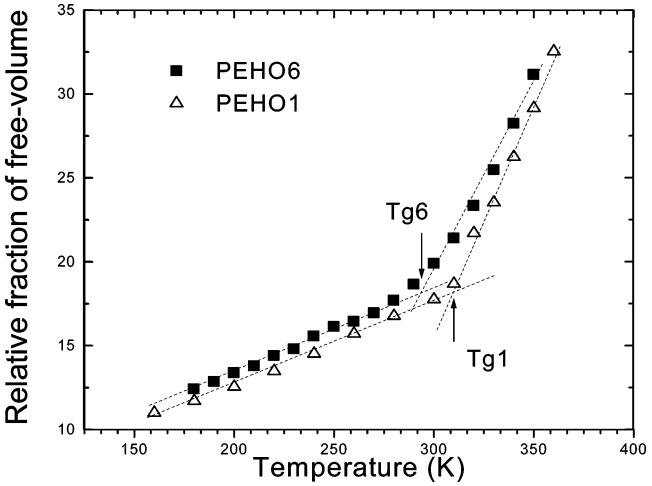

Figure 5. Effect of temperature on apparent free-volume fraction.

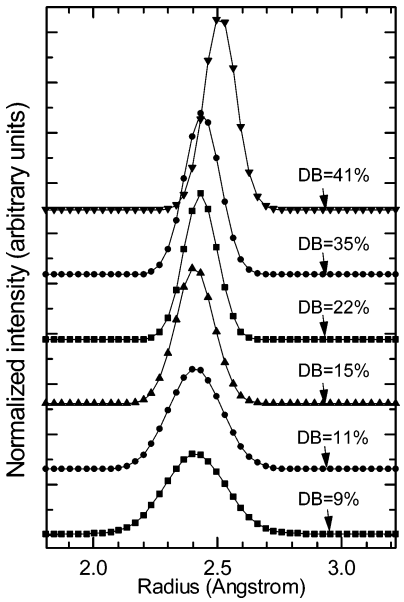

Figure 6. Effect of the degree of branch on free-volume size distrbution for the hyperbranched polymer at room temperature.

volumes are generated more easily in the highly branched PEHO at the same temperature. From Figures 3 and 4, the effect of DB on the free-volume size is very small compared with that on free-volume concentration, because of the restriction of vigorous molecular motion of the backbone chains due to many branching points.

Thus, we can come to the conclusion that the effect of DB on the nanoscale microstructure of hyperbranched polymer PEHO are mainly focus on the numerical concentration of free-volume holes rather than hole size due to the different average chain length between branching points around where o-Ps may be localized and annihilated.

Effect of DB on Free-Volume Size Distribution. To carefully investigate the effect of DB on the free-volume property, positron annihilation lifetime spectra with four million counts were measured at room temperature. Using eq 1, the lifetime distributions were converted in the free-volume size distribution of these six polymers with different DB as shown in Figure 6. Some useful parameters, radius of free volume, R, and intensity of free-volume hole, I, can be calculated as the mass center and as the relative area under the corresponding peak, respectively. Parameters of each peak are given in Table 2, and it is obvious that the position of each peak maintained a constant value of about 2.41 Å except for DB = 41%, while the relative intensity increases dramatically with increasing DB; this is inconsistent with an increase in concentration of free-volume holes. Therefore, we conclude that DB mainly effects the number of the free-volume holes rather than the size. This result is in good agreement with those analyzed by PATFIT.

Table 2. Parameters of the Size Distribution

sample name	area	center position (Å)	fwhm (Å)	height of peak
PEHO1	0.686 17	2.4099	0.245 35	0.031757
PEHO2	0.746 70	2.4100	0.213 69	0.040042
PEHO3	0.755 82	2.4083	0.155 45	0.054037
PEHO4	0.779 22	2.4312	0.135 69	0.058112
PEHO5	0.850 11	2.4378	0.144 03	0.064436
PEHO6	0.975 70	2.5103	0.128 81	0.077319

It should be noticed that the fwhm of distribution decreases gradually with increasing DB. We think that the decrease of the width of the free-volume radius distribution results from the nanoscopic inhomogeneity of PEHO samples, which is quit different for them owing to the effect of DB. With increasing DB, there might be a disappearance of the dynamic heterogeneity in highly branched PEHO and a transition to homogeneous mass takes place. It might be, however, also simply the consequence of the smearing in the molecule and electron density distribution due motional processes with relaxation times near or below the o-Ps lifetime. Maybe the narrow distribution of size observed is due to the increase of segmental chain movements with an increase in DB at fixed temperature.

Effect of Temperature on o-Ps Lifetime Distribution. To carefully investigate how temperature affects the microstructure of PEHO, positron annihilation lifetime spectra with four million counts were collected for three typical samples—PEHO2, PEHO4, and PHEO6, at 200, 290, and 320 K, respectively. Results of continue analysis using MELT program are shown in Figures 7−9. To ensure the reliability of data fitting, calculations of all the continuous positron lifetimes are based on the same conditions.

From Figures 7−9, it is clear that when polymers are in glassy states ($T \leq 290$ K), the lifetime−intensity distribution shows three well-separated peaks. Obviously, the peak of the third component has a strong shift to higher value with increasing temperature, which results from the expansion of free-volume hole.

Above T_g, polymers are in rubbery states, four lifetime components were observed for PEHO2, PEHO4, and PEHO6, and the splitting of the o-Ps lifetime distribution into two subpeaks as temperature is raised has been observed by Ito[33] and Wästlund,[34] which indicates that there are different capture states existing for o-Ps atoms. The fourth component, $\tau_4 \approx 2.25$ ns, is due to o-Ps pick-off annihilation in free-volume holes of the amorphous phase. The nature of the third component ($\tau_3 \approx 1.3$ ns), however, is not very clear. This component does not appear in completely amorphous polymers[35−37] but may be observed in molecular crystals[38,39] and in semicrystalline polymers.[40−44] According to reports mentioned above, maybe the third component arises from o-Ps pick-off annihilation in the interstitial free volume of the crystalline region. The presence of the two o-Ps

Table 3. o-Ps Parameters by PATFIT and MELT for PEHO6 with Temperature

	PATFIT			MELT							
T (K)	τ_3 (ps)	R (Å)	I_3 (%)	τ_3 (ps)	R (Å)	I_3 (%)	τ_4 (ps)	R (Å)	I_4 (%)	τ_{av} (ps)	R_{av} (Å)
200	1478.2	2.312	25.82	1433.3	2.259	26.3				1433.3	2.259
290	1701.2	2.557	26.63	1720.3	2.577	27.0				1720.3	2.577
320	1971.9	2.821	24.78	1172.4	1.92	2.7	2056.5	2.899	20.5	1953.1	2.8052

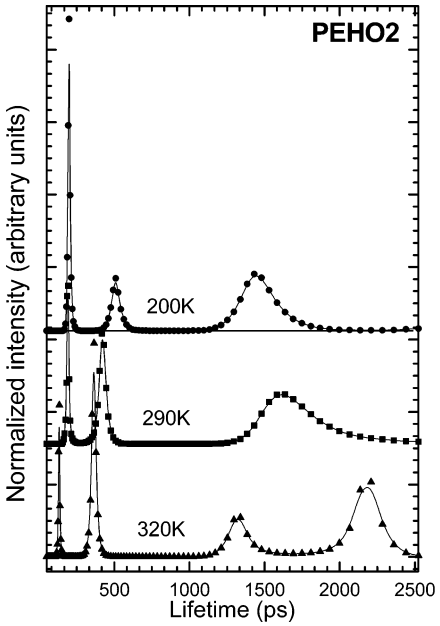

Figure 7. Temperature dependence of the lifetime distribution of positron and positronium for PEHO2.

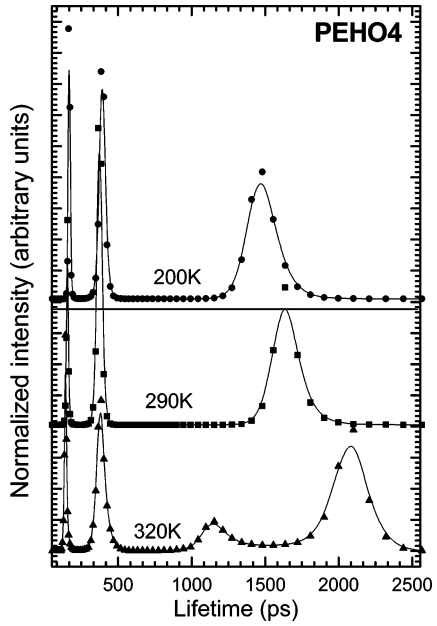

Figure 8. Temperature dependence of the lifetime distribution of positron and positronium for PEHO4.

lifetime values (τ_3 and τ_4) in the rubbery state may be attributed to the unique molecular segment architecture of PEHO as $T > T_g$. A possible explanation to this phenomenon is that there has a very effective rearrangement of chains taking place with activated micro-Brownian motion of whole segments, which results in a tremendous variation in the packing density of chains and the formation of paracrystalline regions where interstitial free volume can be provided for o-Ps to be localized and annihilated inside.

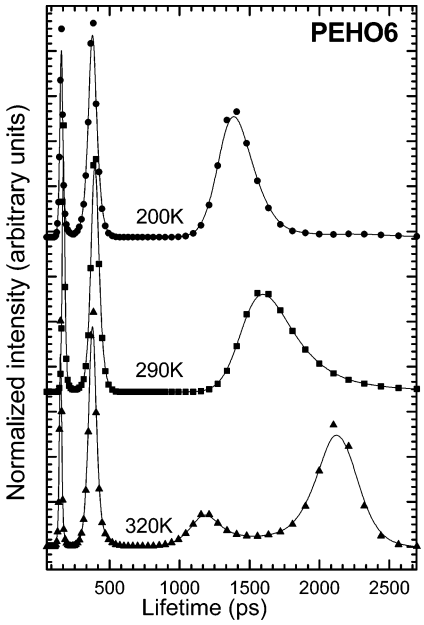

Figure 9. Temperature dependence of the lifetime distribution of positron and positronium for PEHO6.

Table 4. Parameters of the Third Component for Different Samples at T = 320K

sample name	area	fwhm (ps)	height	DB (%)
PEHO2	3.2781	116.87	0.025794	11
PEHO4	3.4423	164.19	0.016728	22
PEHO6	3.9899	248.51	0.012810	41

It is well-known that PATFIT analysis can basically give us the average value of positron annihilation lifetime, and details of lifetime and intensity distribution can be revealed using MELT analysis. The average value of the o-Ps lifetime can be derived from the MELT analysis using the following equation: $\tau_{ave} = (\tau_3 I_3 + \tau_4 I_4)/(I_3 + I_4)$. We have listed the o-Ps lifetimes τ_3, τ_4 and corresponding free-volume radii and their intensities I_3, I_4 analyzed by PATFIT and MELT in Table 3, respectively.

From Table 3, one can see the average o-Ps lifetime and intensity obtained by the MELT program are in good agreement with those by the PATFIT program.

The positron lifetime spectra by MELT analysis provide us some useful information on the widths of distributions of the third component. As listed in Table 4, it shows strongly DB dependence on the characteristic parameters of the third component; both the value of fwhm and the area of the third component increase gradually when the height of each peak decreases with DB increasing. This phenomenon is in good agreement with the crystalline process observed by others,[45] that is, as DB increased, it seems reasonable to believe that the polymer's ability to crystallize decrease, i.e., the higher the DB, the less the linear units, which suggests that the linear units may play an important role in the formation of paracrystalline regions that result from the

variation of packing density of chains. Further studies are in progress.

Conclusion

Positron annihilation lifetime (PAL) measurements have been performed. For highly branched polymers PEHO, the effects of degree of branching (DB) and temperature on the atomic-scale free-volume properties and the structural transitions have been studied. According to the finite-term positron lifetime analysis and differential scanning calorimeter (DSC) measurements, the glass transition temperature was determined, which indicates that the higher the DB, the lower the glass transition temperature, and the higher the concentration of free-volume hole. Both MELT and PATFIT analyses reveal that effects of the degree of branching focus mainly on numerical concentration of nanoscale free-volume rather than on free-volume size. Change in dispersion of the free volume shows that, with DB increase, there might be a disappearance of the dynamic heterogeneity in highly branched PEHO and a transition to homogeneous mass can take place. It is very interesting to observe the existence of two long-lived components above T_g using the continuous lifetime analysis, which suggests that two kinds of different structures appear, including a local ordered region and an amorphous region due to the molecular chains motion, indicating that an effective rearrangement of chains can take place, i.e., paracrystalline regions formed above T_g related to the packing density of chains.

Note Added after ASAP Publication. The version of this paper released ASAP on September 7, 2005, had incorrect author attributions and was withdrawn from the Web on September 13, 2005. The version with full authorship and affiliations was posted on October 20, 2005.

Acknowledgment. This work is financially supported by the National Natural Science Foundation of China, the Basic Research Funds of Shanghai Science and Technique Committee, and the Key Laboratory of Nuclear Solid State Physics of Hubei Province.

References and Notes

(1) Newkome, G. R. *Advances in dendritic molecules, 1*; JAI Press: Greenwich, CT, 1994.
(2) Newkome, G. R.; Moorefield, C. N.; Vögtle, F. *Dendritic molecules: concepts, syntheses, perspectives*; VCH Publishers: New York, 1996.
(3) Gao, C.; Yan, D. *Prog. Polym. Sci.* **2004**, *29*, 183.
(4) Li, X. R.; Zhang, J.; Li, Y. *Macromolecules* **2004**, *37*, 7584.
(5) Peter. J.; Gittins, J.; Alston, Y. Ge, *Macromolecules* **2004**, *37*, 7428.
(6) Unal, S.; Yilger, I.; Yilger, E.; Sheth, J. P. *Macromolecules* **2004**, *37*, 7081.
(7) Yaning He; Xiaogong wang; Qixiang Zhou. *Synth. Met.* **2003**, *132*, 245−248.
(8) Durairaj Baskaran, *Polymer* **2003**, *44*, 2213−2220.
(9) Gao, C.; Yan, D.; Chen, W. *Macromol. Rapid Commun.* **2002**, *23*, 465.
(10) Brandt, W.; Berko, S.; Walker, W. W. *Phys. Rev.* **1960**, *120*, 1280,.
(11) Shrader, D. M.; Jean, Y. C., Eds. *Positron and Positronium Chemistry*; Elsevier: Amsterdam, 1988.
(12) Wang, Cai-lin; Maurer, Frans H. J. *Macromolecules* **1996**, *29*, 8249−8253.
(13) Hristov, H. A.; Bolan, B.; Yee, A. F.; Xie, L.; Gidley, D. W. *Macromolecules* **1996**, *29*, 8507.
(14) Pethrick, R. A. *Prog. Polym. Sci.* **1997**, *22*, 1.
(15) Mai, Y.; Zhou, Y.; Yan, D. *Macromolecules* **2003**, *36*, 9667.
(16) Hawker, C. J.; Lee, R.; Fréchet, J. M. J. *J. Am. Chem. Soc.* **1991**, *113*, 4583.
(17) Mai, Y.; Zhou, Y.; Yan, D.; Hou, J. *New J. Phys.* **2005**, *7*, 42.
(18) Mai, Y.; Zhou, Y.; Yan, D. *Chem. J. Chin. Univ.* **2004**, *25*, 1373.
(19) Kikegaard, P.; Eldrup, M.; Mogensen, O.; Pertersen, N. J. *Comput. Phys. Commun.* **1981**, *23*, 307.
(20) Wästland, C.; Maurer, F. H. *Macromolecules* **1997**, *30*, 5870.
(21) Dammert, R. M.; Maunu, S. L.; Maurer, F. H. J. *Macromolecules* **1999**, *32*, 1930.
(22) Süvegh, K.; Klapper, M.; Domján, A.; Mullins, S. *Macromolecules* **1999**, *32*, 1147.
(23) Tao, S. J. *J. Chem. Phys.* **1972**, *56*, 5499.
(24) Nakanish, H.; Wang, S. J.; Jean, Y. C. World Science: Singapore, 1988; 292.
(25) Lin, D.; Wang, S. J. *J. Phys. Condens. Matter* **1992**, *3*, 333.
(26) Jean, Y. C. *Microchem. J.* **1990**, *42*, 72.
(27) Schrader, D. M.; Jean, Y. C. *Positron and Positronium Chenmistry*; *Positron and Positronium Chemistry*; Schrader, D. M., Jean, Y. C., Eds.; Studies in Physical and Theoretical Chemistry 57, Elsevier: Amsterdam, 1988.
(28) Kobayshi, Y.; Zheng, W.; Meyer, E. F. *Macromolecules.* **1989**, *22*, 2302.
(29) Cangialosi, D.; Schut, H.; Vanveen, A.; Pickem, S. J. *Macromolecules* **2003**, *36*, 142.
(30) Kluin, J. E.; Yu, Z.; Vleeshouwers, S.; McGervey, J. D. *Macromolecules.* **1992**, *25*, 5089.
(31) Consolati, G.; Kansy, J. *Polymer* **1998**, *39*, 3491.
(32) Bartoš, J.; Kirštiaková, K.; Šauša, O *Polymer* **1996**, *15*, 3397.
(33) Ito, K.; Ujihira, Y. *Polymer* **1999**, *40*, 4315.
(34) Wästlund, C.; Maurer, F. H. J. *Macromolecules* **1997**, *30*, 5870.
(35) Jean, Y. C. Positron Annihilation, Proceedings of the 10th International Conference. *Mater. Sci. Forum* **1995**, 175−178.
(36) Nakanishi, H.; Jean, Y. C.; Wang, S. J. *Positron and Positronium Chemistry*; Schrader, D. M., Jean, Y. C., Eds.; Studies in Physical and Theoretical Chemistry 57, Elsevier: Amsterdam, 1988; p 159.
(37) Wang, S. J.; Jean, Y. C. *Positron and Positronium Chemistry*; Schrader, D. M., Jean, Y. C., Eds.; Studies in Physical and Theoretical Chemistry 57, Elsevier: Amsterdam, 1988; p 255.
(38) Lightbody, D.; Sherwood, J. N.; Eldrup, M. *Chem. Phys.* **1985**, *94*, 475.
(39) Eldrup, M. In *Positron Annihilation, Proceedings of the 6th International Conference*; Coleman, P. G., Sharma, S. C., Diana, L. M., Eds; North-Holland: Amsterdam, 1982; p 753.
(40) Dlubek, G.; Saarinen, K.; Fretwell, H. M. *J. Polym. Sci., Part B: Polym. Phys.*, in press.
(41) Dlubek, G.; Saarinen, K.; Fretwell, H. M. *Nucl. Instrum. Methods B* **1998**, in press.
(42) Brauer, G.; Daniel, T.; Faust, W.; Michno, Z. Proceedings of the 4th Int. Workshop on Positron and Positronium Chemistry. *J. Phys. IV (Paris)* **1994**, *3*, *C4*, Suppl. II, no. 9, p 279.
(43) Serna, J.; Abbe, J. C.; Duplatre, G. *Phys. Status Solidi A* **1989**, *115*, 389.
(44) Reiter, G.; Kindl,P. *Phys. Status Solidi A* **1990**, *118*, 161.
(45) Magnusson, H.; Malmström, E.; Hult, A.; Johansson, M. *Polymer* **2002**, *43*, 301.

MA051026J